Author/s:
Clutterbuck, KM;Abrahams, BF;Hudson, TA;van Koeverden, MP

Title:
Mixed valency in a neutral 1D Fe-chloranilate coordination polymer

Date:
2022-06-07

Citation:
Clutterbuck, K. M., Abrahams, B. F., Hudson, T. A. & van Koeverden, M. P. (2022). Mixed valency in a neutral 1D Fe-chloranilate coordination polymer. Dalton Transactions, 51 (24), pp.9199-9205. https://doi.org/10.1039/d1dt04368d.

Persistent Link:
https://hdl.handle.net/11343/324307

Mixed valency in a neutral 1D Fe–chloranilate coordination polymer†

Katelyn M. Clutterbuck,[a] Brendan F. Abrahams,*[a] Timothy A. Hudson,[a] and Martin P. van Koeverden[a,b]

[a]School of Chemistry, University of Melbourne, Parkville, Victoria 3010, Australia.

[b]Present Address: School of Chemistry, The University of Sydney, Sydney, New South Wales 2006, Australia.

†Electronic supplementary information (ESI) available: Synthetic procedures, electrical conductivity measurements and data, general crystallographic details, powder XRD patterns and data, additional structural figures and absorption spectra. CCDC 2131544-2131547. For ESI and crystallographic data in CIF or other electronic format see DOI: 10.1039/****.

The syntheses and structures of a pair of neutral one-dimensional (1D) Fe–anilate based coordination polymers, Fe(Fan)(4,4'-bipy)$_2$ (Fan^{n-} = deprotonated 3,6-difluoro-2,5-dihydroxy-1,4-benzoquinone; 4,4'-bipy = 4,4'-bipyridine) and Fe(Clan)(OPPh$_3$)$_2$ (Clan^{n-} = deprotonated 3,6-dichloro-2,5-dihydroxy-1,4-benzoquinone; OPPh$_3$ = triphenylphosphine oxide), are reported. In the case of Fe(Fan)(4,4'-bipy)$_2$, the Fe centre is in the +2 oxidation state and the Fan ligand is present in its quinoidal, dianionic form. In contrast, the structurally similar Fe(Clan)(OPPh$_3$)$_2$ chain contains Fe centres and chloranilate ligands in oxidation states close to +3 and −3 respectively at low temperature. It is suggested that intrachain π-π interactions aid electron transfer from the Fe centres to the bridging ligands.

Tetraoxolene ligands derived from 2,5-dihydroxy-1,4-benzoquinone (H_2dhbq) have been widely investigated due to their ability to bridge metal centres and therefore generate a rich variety of 1-, 2- and 3-dimensional (1D, 2D and 3D respectively) coordination polymers.[1] When combined with certain metals, the *bis*-bidentate ligands provide a potential pathway for electronic communication between metal centres leading to magnetic ordering and semiconductor behaviour.[2] The nature of the substituents at the 3,6-positions allows the extent of this communication to be tuned.[3] When H_2dhbq and the 3,6-disubstituted derivatives (anilic acid, H_2Xan, X = F, Cl, Br, I, CN etc.), undergo deprotonation they are able to exist in three readily accessible redox states: a quinoid dianion (dhbq^{2-}/Xan^{2-}), a semiquinoid radical trianion (dhbq$^{3-\bullet}$/Xan$^{3-\bullet}$) and an aromatic tetraanion (dhbq^{4-}/Xan^{4-}). In most tetraoxolene coordination polymers, the ligands exist in the dianionic form (dhbq^{2-}/Xan^{2-}).[3–10] The radical trianionic form within coordination polymers is accessible when Xan^{2-} is combined with redox-active metal ions such as Fe(II), affording materials with Xan$^{3-\bullet}$ and Fe(III) valence states.[11,12] To date this behaviour has only been observed in anionic coordination polymers. The radical ligand mediates strong magnetic coupling between metal centres which in turn fosters long-range magnetic ordering.[13,14] In addition to the formal −2 and −3 and oxidation states exhibited

by the ligands, it is not unusual for the tetraoxolenes to exhibit an intermediate oxidation state. In fact, the best performing tetraoxolene-based coordination polymers, with respect to electrical conductivity, tend to be those in which the ligands have non-integer oxidation states i.e. mixed-valence systems.[11,14,15] The presence of mixed valency results in low-energy long range charge transport.[16,17]

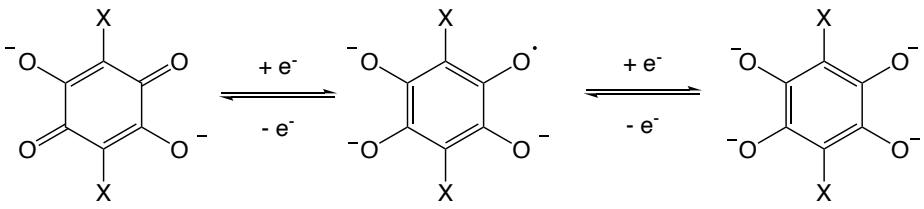

Interest in the conductivity, magnetic ordering and redox switching exhibited by these coordination polymers intensified following Long and co-workers' investigation into $(NBu_4)_2[Fe^{III}_2(dhbq)_3]$,[11] which consists of two interpenetrating three-dimensional (3D) networks each of (10,3)-*a* topology.[18] In this structure, all dhbq ligands are related by crystallographic symmetry and may be formally assigned an oxidation state of −2.67. Crystals of $(NBu_4)_2[Fe^{III}_2(dhbq)_3]$ display a relatively high level of conductivity, with a value of 0.16 S cm^{-1}, placing it amongst the most highly conducting 3D coordination polymers. The oxidation states of the dhbq and the Fe centre contrast with that observed for the isostructural compounds, $(NBu_4)_2[M_2(dhbq)_3]$ (M = Mn, Co, Ni, Zn and Cd) in which the dhbq clearly exists as the quinoidal dianion and the metal is in the +2 oxidation state.[11,18] In an investigation of a similar system, Harris and co-workers described a 2D honeycomb type network of composition $(Me_2NH_2)_2[Fe_2(Clan)_3]$ in which Fe is in the +3 oxidation state and the chloranilate has an average oxidation state of −2.67.[12] These initial reports have spurred significant interest in the conductive and magnetic properties of mixed-valence anionic Fe–tetraoxolene coordination polymers.[7,14,15,19–23] The structural work on these systems has highlighted the impact of countercations on topology and geometry.[2]

The electrically conducting coordination polymers described above, containing ligand-based mixed valency, are examples of 2D and 3D anionic networks. With a view to creating a magnetic 1D coordination polymer, Harris and co-workers[24] synthesised the anionic 1D chain polymer, $(NMe_4)_2[Fe(Clan)Cl_2]$. The chain exhibits thermally-induced valence tautomerism switching between a Fe^{II}-$Clan^{2-}$ state at high temperature, to a Fe^{III}-$Clan^{3-\bullet}$ state at low temperature. At ambient temperature a conductivity of 5.7×10^{-8} S cm^{-1} was measured. Other reported 1D Fe–tetraoxolene structures are neutral and do not exhibit ligand-based mixed valency. These are mainly $Fe(Xan)(H_2O)_2$ type structures, in which a *trans* configuration of water molecules yields a linear ribbon-like polymer, whilst the *cis* arrangement gives rise to a zig-zag polymer.[1,4,25] Apart from the $Fe(Xan)(H_2O)_2$ structures, the only neutral Fe–tetraoxolene coordination polymer is Fe(Clan)(pyrazine).[26] Whilst not crystallographically confirmed, the structure of Fe(Clan)(pyrazine) was proposed to resemble Kitagawa's Cu(Clan)(pyrazine) 2D sheet.[8] These neutral Fe–tetraoxolene coordination polymers (both 1D and 2D) do not exhibit mixed valency, containing only Fe(II) and $Clan^{2-}$ valence states.

We are interested in investigating whether a neutral coordination polymer of composition, $Fe(Xan)L_2$ (L = a neutral co-ligand) can be obtained in which there is evidence for at least some degree of electron transfer from the Fe(II) centre to the tetraoxolene ligand. In the case of $(NMe_4)_2[Fe(Clan)Cl_2]$, coordination of the chlorido anions in addition to the chloranilate anions appears to stabilise the Fe(III) centre. The work described in this report aims to determine whether the choice of appropriate neutral ligands can encourage electron transfer from the Fe(II) centre to a bridging tetraoxolene ligand. Herein, we present a pair of 1D Fe–tetraoxolene coordination polymers incorporating the neutral co-ligands 4,4'-bipyridine (4,4'-bipy) and triphenylphosphine oxide ($OPPh_3$).

Black needles of $Fe(Fan)(4,4'\text{-bipy})_2$ were synthesised by layering an aqueous solution of 4,4'-bipyridine and iron(II) sulfate below a MeOH solution of H_2Fan and allowing the solutions to mix slowly over a period of seven days. Single-crystal X-ray diffraction (SC-XRD) indicated the

formation of a chain structure in which Fe centres are linked by a pair of bridging chloranilate ligands. Two non-bridging 4,4'-bipy ligands complete the octahedral environment around the Fe centre. The 1D polymer is a zig-zag chain, in which the configuration of the Fe centres alternates between Δ and Λ along the length of the polymer (Figure 1a). Comparison of the Fan^{n-} ligand bond lengths in $Fe(Fan)(4,4'\text{-bipy})_2$ with the corresponding bond lengths in $(NEt_4)_2[Zn_2(Fan)_3]$ and $(NBu_4)_2[Zn_2(Fan)_3]$, where the bridging ligand is unambiguously present as Fan^{2-}, indicate that the Fan ligand is in the −2 oxidation state within $Fe(Fan)(4,4'\text{-bipy})_2$.[10,19] The Fe–O bond lengths of 2.092(1) Å and 2.163(1) Å and a Fe-N bond length of 2.153(1) Å are indicative of Fe(II) which is required to balance the charge in this neutral coordination polymer.

a)

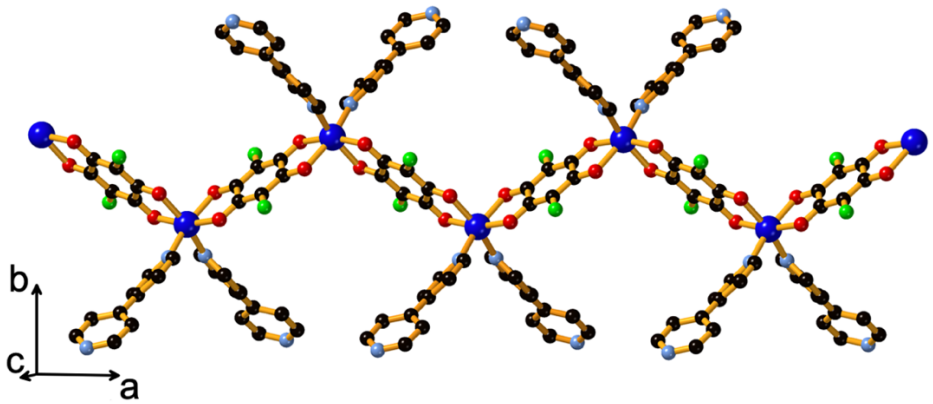

b)

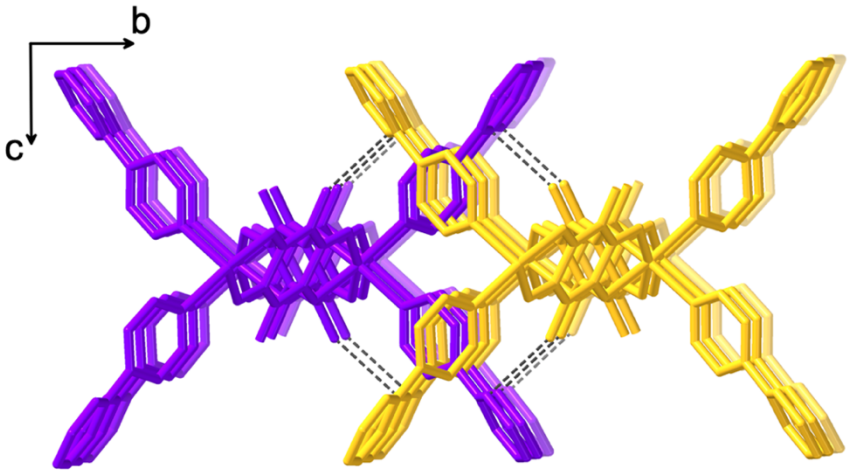

Figure 1: The structure of $Fe(Fan)(4,4'\text{-bipy})_2$ showing a) a single chain with alternating Λ and Δ Fe centres; Fe = royal blue, C = black, N = light blue, O = red, F = green, b) three parallel chains within one layer with interdigitation of 4,4'-bipy ligands; dotted lines indicate F···C contacts between chains.

Parallel chains of Fe(Fan)(4,4'-bipy)$_2$ extending in the *a*-direction form a layer in the *a*-*b* plane, with the closet interchain contacts occurring between F atoms of the Fan^{2-} ligands and C atoms of the non-coordinated pyridyl ring of the 4,4'-bipy ligands (Figure 1b). The C···F separation is 2.991(2) Å and each chain forms an infinite number of such interactions along the length of the *a*-axis with the two neighbouring chains. Parallel layers stack along the *c*-direction in an ABAB… arrangement with the non-coordinated 4,4'-bipy ligands from adjacent layers interdigitating (Figure S4). Crystals of the analogous Zn(II) compound were formed under similar synthetic conditions, however it was not possible to obtain phase-pure Zn(Fan)(4,4'-bipy)$_2$. A crystal structure determination on isolated crystals of Zn(Fan)(4,4'-bipy)$_2$ indicated essentially the same structure as the Fe analogue, with fluoranilate present in its expected Fan^{2-} form.

Triphenylphosphine oxide (OPPh$_3$) is an example of a hard donor ligand known to promote crystallisation.[27] It was selected as a co-ligand for the Fe–chloranilate system primarily because it was thought it could assist in stabilising Fe(III). A common method to generate crystalline metal-tetraoxolene coordination polymers involves the use of the reduced form of the ligands i.e. 3,6-disubstituted-1,2,4,5-tetrahydroxybenzene (H$_4$Xan; X= F, Cl, Br etc.) as a starting material.[10,18,28,29] Using this approach, the coordination polymer, Fe(Clan)(OPPh$_3$)$_2$, was synthesised by layering an aqueous solution of iron(II) sulfate below an acetone solution of OPPh$_3$ and H$_4$Clan. Black needles suitable for SC-XRD formed just above the interface of the layers after slow diffusion. An X-ray diffraction study conducted on a crystal at 100 K afforded a structure solution in the monoclinic space group *P*2/*c*. Octahedral Fe centres are bridged by chloranilate ligands to form zig-zag chains (Figure 2). The coordination environment of the Fe is completed by a pair of *cis* OPPh$_3$ ligands. A 2-fold axis, normal to the direction of the chain and parallel to the *b* axis, passes through each Fe centre and each chloranilate ligand is located on a centre of inversion. The individual zig-zag chains, which are all parallel, resemble the 1D coordination polymer, Fe(Fan)(4,4'-bipy)$_2$ and indeed the previously reported, Fe(Clan)(H$_2$O)$_2$·H$_2$O.[4] The Fe···Fe···Fe angle in the zig-zag chain is 108.9° compared to

126.3° and 118.3° in Fe(Clan)$(H_2O)_2 \cdot H_2O$ and Fe(Fan)(4,4'-bipy)$_2$ respectively. The relatively small Fe···Fe···Fe angle presumably reflects the steric demands of the $OPPh_3$ ligands. Only weak interactions exist between parallel chains with the closest separation involving a phenyl proton from a $OPPh_3$ ligand on one chain forming a C–H···O hydrogen bond (3.49 Å) with a chloranilate oxygen atom in an adjacent chain. Each chain acts as a multiple donor and acceptor in such interactions with equivalent parallel chains on either side, forming a sheet-like structure in which all metal atoms of the chains are co-planar (Figure S5).

Whilst the aforementioned synthetic process yields good quality crystals suitable for single crystal X-ray diffraction, the bulk crystalline product was found to be contaminated. An alternative synthetic approach, described in detail in the ESI, using chloranilic acid, ammonium iron(II) sulfate hexahydrate, triphenylphosphine oxide and sodium hydrogen sulfite yielded a phase pure bulk product as indicated by powder X-ray diffraction and microanalysis.

a)

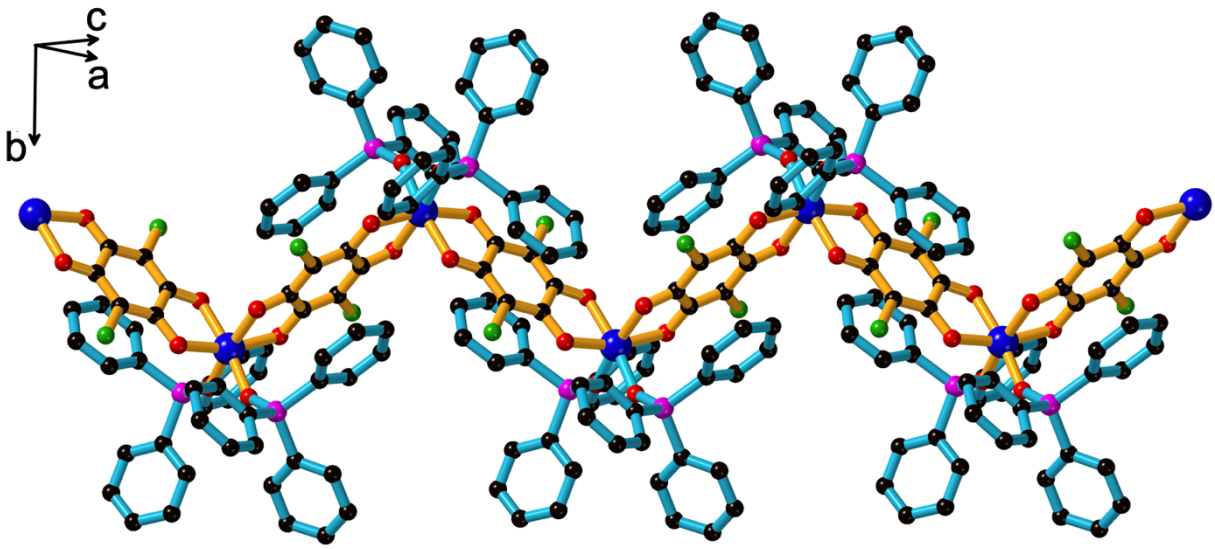

b)

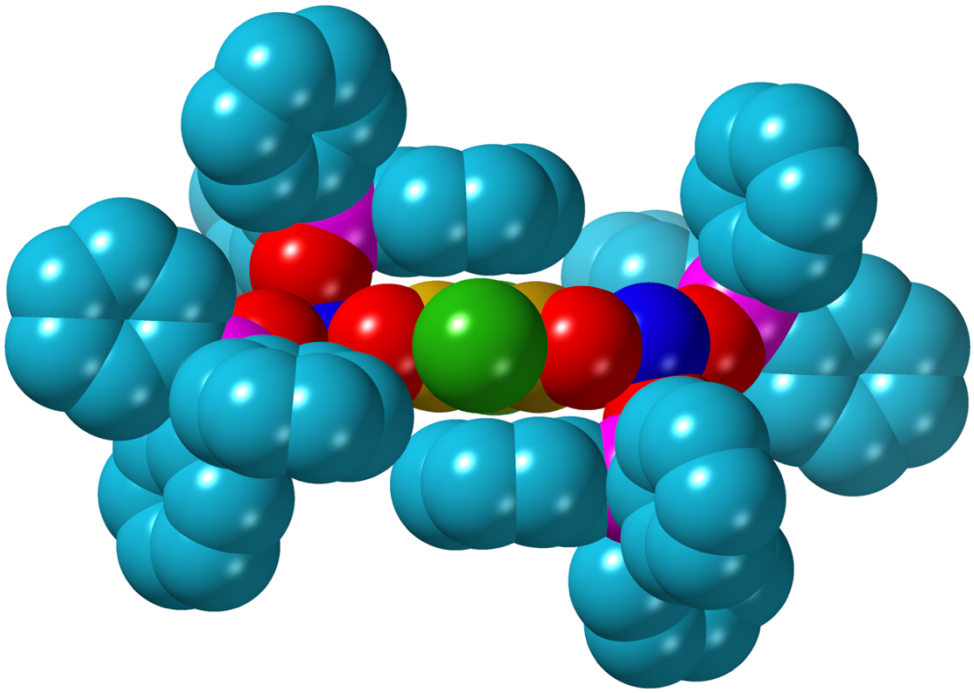

Figure 2: The structure of Fe(Clan)($OPPh_3$)$_2$ showing a) part of a single chain Fe = blue, C = black, O = red, P = pink, Cl = green; b) a space-filling representation of a section of the 1D polymer with $OPPh_3$ phenyl groups (turquoise) flanking the bridging chloranilate ligand; Fe = blue, C = gold (chloroanilate), O = red, P = pink, Cl = green.

Analysis of bond lengths indicate a difference in the Fe and chloranilate oxidation states within $Fe(Clan)(OPPh_3)_2$ compared with $Fe(Fan)(4,4'\text{-bipy})_2$ and other neutral Fe–tetraoxolene coordination polymers. A comparison of bond lengths in $Fe(Clan)(OPPh_3)_2$ (at 100 and 300 K), $Fe(Fan)(4,4'\text{-bipy})_2$ and $Fe(Clan)(H_2O)_2$ is presented in Figure 3. The average OC–CO length in $Fe(Clan)(OPPh_3)_2$ is 1.497(3) Å which is shorter than commonly observed for $Clan^{2-}$ (1.506-1.551) but slightly longer than typically found for $Clan^{3-\bullet}$.[22] Similarly, the average C–O bond length of 1.28 Å is intermediate between that typically expected for $Clan^{2-}$ and $Clan^{3-\bullet}$ when acting as bridging ligands.[22] For comparative purposes, ligand bond lengths for Fe–tetraoxolene systems are presented in Table 1 along with the assigned valency of the ligand. The bond lengths in $Fe(Clan)(OPPh_3)_2$ are thus consistent with an oxidation state for the chloranilate intermediate between −2 and −3. In order to maintain neutrality, the magnitude of the charge on the chloranilate needs to match the charge on the Fe centre and indeed, the relatively short Fe–O(chloranilate) bond lengths of 2.051(2) and 2.014(2) Å are indicative of an oxidation state close to Fe(III).[22] The longer Fe–O (chloranilate) bonds are *trans* to the $OPPh_3$ ligands. The Fe–O ($OPPh_3$) bond length of 2.008(2) Å is also close to that expected for Fe(III).[30,31]

The structural results indicate a significant degree of electron transfer from the Fe(II) centre to $Clan^{2-}$. Bond valence sum calculations[32] suggest an oxidation state of +2.9 for the Fe centre. When the structure determination is performed on data recorded at 300 K, an increase in Fe–O(chloranilate) bond lengths is noted (2.098(2) and 2.043(2) Å) and is accompanied by changes in C–O and diagnostic C–C bond lengths of the chloranilate ligands. These changes are consistent with a clear shift towards the $Clan^{2-}$ state for the bridging ligands, but nevertheless, still intermediate between $Clan^{3-\bullet}$ and $Clan^{2-}$. Similarly, elongation of the Fe–O bonds is consistent with a reduction of the Fe towards the +2 oxidation state. Bond valence sum calculations based on the 300 K data indicate an oxidation state of +2.7. The thermally-induced electronic structure change in $Fe(Clan)(OPPh_3)_2$ mirrors that observed in the 1D $(NMe_4)_2[Fe(Clan)Cl_2]$[24] and 2D $(NPr_4)_2[Fe_2(Clan)_3]$.[21] These compounds similarly transition from low-temperature $[Fe^{III}(Clan^{3-\bullet})Cl_2]^{2-}$ or $[Fe^{III}_2(Clan^{2-})(Clan^{3-\bullet})_2]^{2-}$ valence distributions

respectively, to $[Fe^{II}(Clan^{2-})Cl_2]^{2-}$ and $[Fe^{III}Fe^{III}(Clan^{2-})_2(Clan^{3-\bullet})]^{2-}$ valence tautomers at high temperature.

The structure determinations provide an opportunity to speculate upon the reason $OPPh_3$ leads to electron transfer from the Fe centre to the chloranilate. As stated earlier, $OPPh_3$ may be considered a hard donor ligand and is expected to stabilise the Fe(III) state for the Fe centre, however, water, which is also a hard donor ligand, does not appear to have a similar effect. Inspection of the zig-zag structure reveals a phenyl group on each of the coordinated $OPPh_3$ ligands is oriented such that it forms face-to-face π-interactions with one of the $Clan^{n-}$ ($2 < n < 3$) ligands coordinated to the same Fe centre. This leads to each tetraoxolene ligand being sandwiched between a pair of phenyl rings (Figures 2a and b). This arrangement of phenyl rings may assist in stabilising the intermediate oxidation state. The closest C···C contact between the phenyl ring of the $OPPh_3$ and the chloranilate ring is 3.331(5) Å. This interaction may be enhanced by the coordinated phosphine oxide group having an electron withdrawing effect, resulting in electron deficient phenyl groups being able to stabilise an electron rich form of the Clan ligand in which the oxidation state approaches −3. Similar face-to-face interactions have been identified in (PhenQ)$[Fe_2(Clan)_3]$·solvent ($PhenQ^{2+}$= 5,6-dihydropyrazino[1,2,3,4-*lmn*] [1,10]-phenanthrolindiium),[22] where electron-deficient $PhenQ^{2+}$ cations form close π-π stacking interactions with the $Clan^{3-\bullet}$ ligands within a 2D sheet. Within (PhenQ)$[Fe_2(Clan)_3]$, it is believed that the face-to-face π-interaction is responsible for the localisation of the $Clan^{3-\bullet}$ state, rather than delocalisation as observed in $(Me_2NH_2)_2[Fe_2(Clan)_3]$ and $(NEt_4)_2[Fe_2(Clan)_3]$.

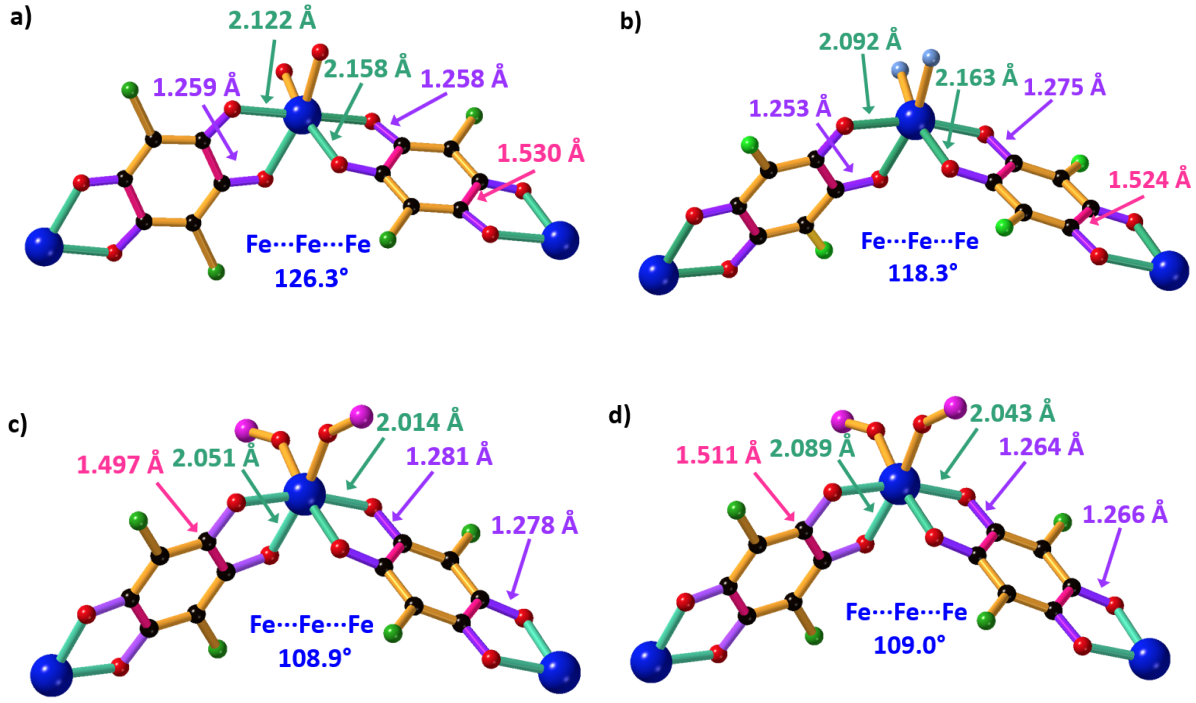

Figure 3: Comparison of relevant bond lengths in **a)** Fe(Clan)$(H_2O)_2$; **b)** Fe(Fan)(4,4'-bipy)$_2$; **c)** Fe(Clan)$(OPPh_3)_2$ (100 K) and **d)** Fe(Clan)$(OPPh_3)_2$ (300 K); C-C bonds pink, C-O bonds purple, Fe-O bonds teal. In each case the anilate ligands are crystallographically equivalent and each is located on a centre of inversion.

Room temperature pressed-pellet conductivity measurements for Fe(Clan)$(OPPh_3)_2$ indicate a conductivity of 1.36×10^{-7} S cm^{-1}. This is much lower than that observed for other 2D and 3D Fe-tetraoxolene based frameworks in which the Clan$^{3-\bullet}$ form is present at least to some extent (Table 1). The lower conductivity is not surprising given that the electrical conductivity is likely to be limited to the direction of the chains, which are randomly oriented in the pressed pellet. The conductivity is slightly higher than in the aforementioned 1D zig-zag coordination polymer $(NMe_4)_2[Fe^{III}(Clan)Cl_2]$.[24]

Solid state absorption spectra (Figure S7) were recorded for both $Fe(Clan)(H_2O)_2 \cdot H_2O$ and $Fe(Clan)(OPPh_3)_2$. The spectrum of $Fe(Clan)(H_2O)_2 \cdot H_2O$ shows two strong broad UV absorbances at 44,500 cm^{-1} (225 nm) and 28,250 cm^{-1} (354 nm). A weaker broad absorption between 20,000 and 10,000 cm^{-1} (500–1000 nm) is apparent. Below 10000 cm^{-1} the measured absorption drops relatively steeply. The spectrum of $Fe(Clan)(OPPh_3)_2$ shares some similarities with $Fe(Clan)(H_2O)_2 \cdot H_2O$, with absorptions at 43,750 cm^{-1} (229 nm) and 26,250 cm^{-1} (381 nm), in addition to a broad absorption in the visible region. Below 10,000 cm^{-1} (1000 nm) there is a significant difference between the spectra with a major absorption for $Fe(Clan)(OPPh_3)_2$ at ~7250 cm^{-1} (1379 nm), suggestive of intervalence charge transfer.[11,19,20,22] The spectrum of $Fe(Fan)(4,4'\text{-bipy})_2$ was also recorded in the UV-Vis-NIR region (Figure S7) and showed major absorbances at 40,380, 28,000, 21,250, 10,500 and 8,500 cm^{-1}. Comparisons of the spectrum for $Fe(Fan)(4,4'\text{-bipy})_2$ with the other two Fe compounds are difficult because of the different bridging ligand and the presence of the coordinated 4,4'-bipy ligand.

To the best of our knowledge $Fe(Clan)(OPPh_3)_2$ is the first example of a neutral Fe–tetraoxolene coordination polymer in which there is evidence for at least partial electron transfer from the metal to the ligand. A summary of 1D, 2D and 3D iron tetraoxolene polymeric structures presented in Table 1, shows that in previously reported structures, electron transfer from Fe(II) to the ligand had only been observed within anionic systems. The ligands bound to the Fe centre in these anionic polymers all possess a formal negative charge, and this likely facilitates electron transfer from the Fe centre to the tetraoxolene ligands. In the case $Fe(Clan)(H_2O)_2 \cdot H_2O$, the Fe centre is unambiguously Fe(II) with an average Fe–O distance of 2.125 Å. The pair of *cis* water molecules coordinated to the Fe(II) centre, in this zig-zag 1D polymer, presumably provide insufficient negative charge to drive electron density from the metal centre to the tetraoxolene ligands. In the case of $Fe(Clan)(OPPh_3)_2$, it may be that the $OPPh_3$ is a sufficiently strong σ-donor to promote the electron transfer. However, as indicated above, the face-on phenyl groups from the $OPPh_3$, may promote the transfer of electron density from metal centre to the tetraoxolene, particularly at low temperature. Clearly further work is

required to confirm whether the $Clan^{3-\bullet}$ state is stabilised by face-to-face associations with phenyl groups. It was hoped that the use of trialkylphosphine oxides as co-ligands in place of $OPPh_3$ could serve to clarify the importance of the π-π interactions, but it has not been possible to obtain crystals with such ligands. If metal-to-ligand electron transfer in Fe–tetraoxolene systems could be controlled by face-to-face interactions between π-delocalised systems and bridging tetraoxolene ligands, physical properties such as electrical conductivity could be modulated by tuning the strength of these non-covalent interactions.

Table 1: Comparison of the presence of mixed valency, relevant bond lengths and ambient temperature electrical conductivity in Fe-tetraoxolene based coordination polymers.

Compound	Dimens-ionality	Fe Ox State	Av. Fe–O (Å)	Anilate Charge	Av. C–O (Å)	Av. C–C (Å)	σ (S cm^{-1})[b]	Ref.
$Fe(Fan)(4,4'\text{-bipy})_2$	1D	2+	2.128(1)	2−	1.264(2)	1.524(1)	-	†
$Fe(Clan)(OPPh_3)_2$ (100 K)	1D	2+/3+	2.033(2)	2−/3−	1.280(3)	1.497(3)	1.36×10^{-7}	†
$Fe(Clan)(OPPh_3)_2$ (300 K)	1D	2+/3+	2.066	2−/3−	1.265	1.511(3)		†
$Fe(Clan)(H_2O)_2 \cdot H_2O$	1D	2+	2.125	2−	1.259(3)	1.530(3)	-	4, 5
$[Fe(H_2O)_2(Clan)] \cdot phz$	1D	2+	2.141	2−	1.262(3)	1.522(4)	-	5
$(Me_4N)_2[FeCl_2(Clan)]$ (100 K)	1D	3+	2.027	3−	1.291(3)	1.466(4)	5.7×10^{-8}	24
$(Me_4N)_2[FeCl_2(Clan)]$ (250 K)	1D	2+	2.140(5)	2−	1.256	1.523(9)		24
$(H_2NMe_2)_2[Fe_2Clan_3] \cdot 2H_2O \cdot 6DMF$	2D	3+	2.020(3)	2.67−	1.280(5)	1.480(9)	$1.4(7) \times 10^{-2}$	12, 14
$(Cp_2Co)_{1.43}(H_2NMe_2)_{1.57}[Fe_2Clan_3] \cdot 4.9DMF$	2D	3+	2.028(6)	3−	1.298(9)	1.431(16)	$5.1(3) \times 10^{-4}$	14
$(NPr_4)_2[Fe_2(Clan)_3] \cdot 2acetone \cdot H_2O$ (103 K)	2D	3+	2.024	3− 2−	1.293(3) 1.296(3) 1.259(3)	1.472(3) 1.468 (3) 1.534	$\sigma_{\parallel}$ 2.6 × 10^{-4} $\sigma_{\perp}$1.0 × 10^{-4}	21
$(NPr_4)_2[Fe_2(Clan)_3] \cdot 2acetone \cdot H_2O$ (241 K)	2D	2+ 3+	2.091(2) 2.034(2)	3− 2−	1.294(4) 1.258(4) 1.266(4)	1.468(4) 1.530(4) 1.518(4)		21
$(NEt_4)_2[Fe_2(Clan)_3] \cdot 20H_2O$	2D	3+	2.018(3)	2.67−	1.284(4)	1.491(6)	-	20
$(NEt_4)_2[Fe_2(Fan)_3] \cdot 5acetone$	2D	3+	2.019(3)	2.67−	1.264(5)	1.497(6)	1.8×10^{-2}	15
$[TAG][Fe_2(ClCNan)_3] \cdot solvate$ [a]	2D	2.5+	2.043(6) 2.046	2−	1.26 1.32*	1.50 1.41*	$\sigma_{\parallel}$ 2 × 10^{-3} $\sigma_{\perp}$ 7 × 10^{-6}	6
$(H_3O)(phz)_3[Fe_2(Clan)_3] \cdot 13H_2O$	2D	2.5+	2.063(2)	2−	1.268(3)	1.529(5)	$\sigma_{\parallel}$ 3 × 10^{-2} $\sigma_{\perp}$ 1 × 10^{-4}	7
$(H_3O)(phz)_3[Fe_2(Bran)_3] \cdot 13H_2O$	2D	2.5+	2.076(3)	2−	1.262(6)	1.534(9)	$\sigma\parallel$ 3 ×10^{-3} $\sigma\perp$ 6 × 10^{-6}	7
$(PhenQ)[Fe_2(Clan)_3] \cdot solvate$	2D	3+	2.029(2)	2.5− 3−	1.274(2) 1.295(2)	1.495(3) 1.464(4)	4.9 × 10^{-4}	22
$(NBu_4)_2[Fe_2(dhbq)_3]$	3D	3+	2.018(7)	2.67−	1.295	1.521(12)	1.6 × 10^{-1}	11

[a]TAG = tris(amino)-guanidinium; [b] $\sigma_{\parallel}$ indicates conductivity parallel to sheet and $\sigma_{\perp}$ indicates conductivity perpendicular to sheet

*Bond lengths within $[TAG][Fe_2(ClCNan)_3] \cdot (solvate)$ are anomalous due to differences in the nature of the tetraoxalene substituents.

† This work.

Acknowledgements

The authors gratefully acknowledge the financial support of the Australian Research Council (DP180101413). This research was undertaken in part using the MX2 beamline at the Australian Synchrotron, part of ANSTO, and made use of the Australian Cancer Research Foundation (ACRF)

detector. The authors gratefully acknowledge Prof. Deanna D'Alessandro of the University of Sydney for spectroscopic measurements.

References

1 S. Kitagawa and S. Kawata, *Coord. Chem. Rev.*, 2002, **224**, 11–34.
2 M. L. Mercuri, F. Congiu, G. Concas and S. A. Sahadevan, *Magnetochemistry*, 2017, **3**, 17.
3 M. Atzori, S. Benmansour, G. Mínguez Espallargas, M. Clemente-León, A. Abhervé, P. Gómez-Claramunt, E. Coronado, F. Artizzu, E. Sessini, P. Deplano, A. Serpe, M. L. Mercuri and C. J. Gómez García, *Inorg. Chem.*, 2013, **52**, 10031–10040.
4 B. F. Abrahams, K. D. Lu, B. Moubaraki, K. S. Murray and R. Robson, *J. Chem. Soc. Dalt. Trans.*, 2000, 1793–1797.
5 S. Kawata, S. Kitagawa, H. Kumagai, T. Ishiyama, K. Honda, H. Tobita, I. Keiichi Adachi and M. Katada, *Chem. Mater.*, 1998, **10**, 3902–3912.
6 S. A. Sahadevan, A. Abhervé, N. Monni, C. Sáenz De Pipaón, J. R. Galán-Mascarós, J. C. Waerenborgh, B. J. C. Vieira, P. Auban-Senzier, S. Pillet, E. E. Bendeif, P. Alemany, E. Canadell, M. L. Mercuri and N. Avarvari, *J. Am. Chem. Soc.*, 2018, **140**, 12611–12621.
7 S. Benmansour, A. Abhervé, P. Gómez-Claramunt, C. Vallés-García and C. J. Gómez-García, *ACS Appl. Mater. Interfaces*, 2017, **9**, 26210–26218.
8 S. Kawata, S. Kitagawa, M. Kondo, I. Furuchi and M. Munakata, 1994, **33**, 1759–1761.
9 B. F. Abrahams, J. Coleiro, K. Ha, B. F. Hoskins, S. D. Orchard and R. Robson, *J. Chem. Soc. Dalt. Trans.*, 2002, **2**, 1586–1594.
10 C. J. Kingsbury, B. F. Abrahams, J. E. Auckett, H. Chevreau, A. D. Dharma, S. Duyker, Q. He, C. Hua, T. A. Hudson, K. S. Murray, W. Phonsri, V. K. Peterson, R. Robson and K. F. White, *Chem. - A Eur. J.*, 2019, **25**, 5222–5234.
11 L. E. Darago, M. L. Aubrey, C. J. Yu, M. I. Gonzalez and J. R. Long, *J. Am. Chem. Soc.*, 2015, **137**, 15703–15711.
12 I. R. Jeon, B. Negru, R. P. Van Duyne and T. D. Harris, *J. Am. Chem. Soc.*, 2015, **137**, 15699–15702.
13 L. Liu, J. A. DeGayner, L. Sun, D. Z. Zee and T. D. Harris, *Chem. Sci.*, 2019, **10**, 4652–4661.
14 J. A. DeGayner, I. R. Jeon, L. Sun, M. Dincă and T. D. Harris, *J. Am. Chem. Soc.*, 2017, **139**, 4175–4184.
15 R. Murase, C. J. Commons, T. A. Hudson, G. N. L. Jameson, C. D. Ling, K. S. Murray, W. Phonsri, R. Robson, Q. Xia, B. F. Abrahams and D. M. D'Alessandro, *Inorg. Chem.*, 2020, **59**, 3619–3630.
16 C. F. Leong, P. M. Usov and D. M. D'Alessandro, *MRS Bull.*, 2016, **41**, 858–864.
17 V. Stavila, A. A. Talin and M. D. Allendorf, *Chem. Soc. Rev.*, 2014, **43**, 5994–6010.
18 B. F. Abrahams, T. A. Hudson, L. J. McCormick and R. Robson, *Cryst. Growth Des.*, 2011, **11**, 2717–2720.
19 R. Murase, B. F. Abrahams, D. M. D'Alessandro, C. G. Davies, T. A. Hudson, G. N. L. Jameson, B. Moubaraki, K. S. Murray, R. Robson and A. L. Sutton, *Inorg. Chem.*, 2017, **56**, 9025–9035.
20 C. J. Kingsbury, B. F. Abrahams, D. M. D'Alessandro, T. A. Hudson, R. Murase, R. Robson and K. F. White, *Cryst. Growth Des.*, 2017, **17**, 1465–1470.
21 J. Chen, Y. Sekine, Y. Komatsumaru, S. Hayami and H. Miyasaka, *Angew. Chem., Int. Ed.*, 2018, **57**, 12043–12047.
22 M. P. van Koeverden, B. F. Abrahams, D. M. D'Alessandro, P. W. Doheny, C. Hua, T. A. Hudson, G. N. L. Jameson, K. S. Murray, W. Phonsri, R. Robson and A. L. Sutton, *Chem. Mater.*, 2020, **32**, 7551–7563.
23 R. Murase, C. F. Leong and D. M. D'Alessandro, *Inorg. Chem.*, 2017, **56**, 14373–14382.
24 J. A. DeGayner, K. Wang and T. D. Harris, *J. Am. Chem. Soc.*, 2018, **140**, 6550–6553.
25 J. T. Wrobleski and D. B. Brown, *Inorg. Chem.*, 1979, **18**, 2738–2749.
26 J. T. Wrobleski and D. B. Brown, *Inorg. Chem.*, 1979, **18**, 498–504.
27 M. C. Etter and P. W. Baures, *J. Am. Chem. Soc.*, 1988, **110**, 639–640.
28 B. F. Abrahams, A. D. Dharma, B. Dyett, T. A. Hudson, H. Maynard-Casely, C. J. Kingsbury,

L. J. McCormick, R. Robson, A. L. Sutton and K. F. White, *Dalt. Trans.*, 2016, **45**, 1339–1344.
29 B. F. Abrahams, A. M. Bond, T. H. Le, L. J. McCormick, A. Nafady, R. Robson, N. Vo, *Chem. Commun*. 2012, **48**, 11422-11424.
30 E. Ďurčanská, T. Głowiak, J. Kožíšek, I. Ondrejkovičová and G. Ondrejovič, *Acta Crystallogr. Sect. C Cryst. Struct. Commun.*, 1989, **45**, 410–412.
31 Z. F. Zhang, *Zeitschrift fur Krist. - New Cryst. Struct.*, 2011, **226**, 486–488.
32 O. C. Gagné and F. C. Hawthorne, *Acta Crystallogr. Sect. B Struct. Sci. Cryst. Eng. Mater.*, 2015, **71**, 562–578.